

Title:

Dissolved methane oxidation and competition for oxygen in down-flow hanging sponge reactor for post-treatment of anaerobic wastewater treatment

Authors:

Masashi HATAMOTO^{a,b,*}, Tomo MIYAUCHI^c, Tomonori KINDAICHI^a, Noriatsu OZAKI^a and Akiyoshi OHASHI^a

Address:

^aDepartment of Civil and Environmental Engineering, Graduate School of Engineering, Hiroshima University, 1-4-1 Kagamiyama, Higashihiroshima, Hiroshima 739-8527, Japan

^b Department of Environmental Systems Engineering, Nagaoka University of Technology, 1603-1, Kamitomiokamachi, Nagaoka, Niigata 940-2188, Japan

^cCivil & Environmental Engineering Program, Faculty of Engineering, Hiroshima University, 1-4-1 kagamiyama, Higashihiroshima, Hiroshima 739-8527, Japan

***Corresponding author:**

Masashi HATAMOTO

Phone: +81- 258-47-9642. Fax: +81- 258-47-9637.

E-mail: hatamoto@vos.nagaokaut.ac.jp

Abstract

Post-treatment of anaerobic wastewater was undertaken to biologically oxidize dissolved methane, with the aim of preventing methane emission. The performance of dissolved methane oxidation and competition for oxygen among methane, ammonium, organic matter, and sulfide oxidizing bacteria were investigated using a lab-scale closed-type down-flow hanging sponge (DHS) reactor. Under the oxygen abundant condition of a hydraulic retention time of 2 h and volumetric air supply rate of $12.95 \text{ m}^3\text{-air}\cdot\text{m}^{-3}\cdot\text{day}^{-1}$, greater than 90% oxidation of dissolved methane, ammonium, sulfide, and organic matter was achieved. With reduction in the air supply rate, ammonium oxidation first ceased, after which methane oxidation deteriorated. Sulfide oxidation was disrupted in the final step, indicating that COD and sulfide oxidation occurred prior to methane oxidation. A microbial community analysis revealed that peculiar methanotrophic communities dominating the *Methylocaldum* species were formed in the DHS reactor operation.

Keywords: Greenhouse gas, Methane oxidation, Anaerobic treatment, Post-treatment, Down-flow hanging sponge (DHS)

1. Introduction

Anaerobic waste/wastewater treatment technology has several advantages over the conventional aerobic treatment system, such as a lower energy requirement and reduced production of excess sludge. In recent years, anaerobic treatment process has been focused not only on its cost-saving advantages but also its eco-friendly nature in terms of the energy recovery as methane gas and reduction in CO₂ emissions. And thus its applications are expanding in various types of wastewaters, including low-strength wastewaters (Kassab et al., 2010; Takahashi et al., 2011). However, the anaerobic process discharges unrecovered methane as dissolved methane in the effluent. Methane is a greenhouse gas with a 25-fold greater effect on global warming than CO₂ (Forster et al., 2007), thus reduction of dissolved methane emission is significantly important for further popularization of anaerobic treatment technologies.

To date, few studies have been conducted on the removal and/or recovery of dissolved methane from anaerobic wastewater treatment. Hartley and Lant (2006) applied microaeration to reduce the dissolved methane effusion. To recover and remove the dissolved methane, Matsuura et al. (2010) employed a two-stage closed down-flow hanging sponge (DHS) reactor; the first DHS reactor recovered the dissolved methane as burnable gas, whereas the second reactor oxidized residual dissolved methane. We have been developing a biological dissolved methane oxidation system using the single closed DHS reactor (Hatamoto et al., 2010), which revealed that methane oxidation occurred preferentially over ammonium oxidation in the reactor; however, the interactions of methane oxidation with sulfide and organic carbon oxidation remain to be investigated. The DHS reactor has been

developing as a low cost post-treatment for the anaerobic treatment process and applied to several types of wastewaters (Machdar and Faisal, 2011; Takahashi et al., 2011; Tandukar et al., 2007); thus, it is a promising method for removing dissolved methane as well as polish up the anaerobically treated effluent.

In this study, in order to clarify the effects of hydraulic retention time (HRT) and air supply rate on methane, ammonium, sulfide, and COD removal, a lab-scale closed DHS reactor was operated using artificial anaerobic wastewater, and the reactor performance was evaluated. Further, the microbial community structure based on the 16S rRNA gene sequence and the succession of methane-oxidizing bacterial communities based on the particulate methane monooxygenase (*pmoA*) gene were also investigated.

2. Materials and Methods

2.1 Experimental set-up and operational conditions

In this study, a closed DHS reactor of a 4 L column (112 cm in height and 6.8 cm in diameter) was used. In the closed DHS reactor, a string of 31 polyurethane sponge-cubes ($2 \times 2 \times 2$ cm in size) connected diagonally in series with each other was hanged. The hanging string of sponge-cubes was 1 m in vertical length with a working volume of 0.25 L, based on sponge volume (Fig.1). To inoculate the sludge, the string of sponge-cubes was soaked in diluted activated sludge from a wastewater treatment plant treating municipal sewage. The artificial wastewater with dissolved methane, which was made by purging artificial wastewater with methane gas (100% [v/v]), was fed into the system from the top of the reactor. The artificial wastewater contained in 1 L: 11 mg KH_2PO_4 ; 5 mg $\text{CaCl}_2 \cdot 2\text{H}_2\text{O}$; 33

mg $\text{MgCl}_2 \cdot 6\text{H}_2\text{O}$; 16 mg KCl; 150 mg NH_4Cl ; 40.5 mg Na_2S ; 25 mgCOD propionate; and 25 mgCOD acetate. The trace elements solution was added at the previously described concentration (Hatamoto et al., 2010). The pH in the feed was maintained at 8.1 by addition of $500 \text{ mg} \cdot \text{L}^{-1} \text{NaHCO}_3$. The reactor was maintained at 20°C and was operated as shown in Table 1.

2.2 Analytical methods

The concentrations of NH_4^+ , NO_2^- , NO_3^- , and SO_4^{2-} were routinely measured by ion chromatography (Hatamoto et al., 2010). COD was analyzed using an HACH water quality analyzer (HACH DR4000). For measurement of effluent COD, a small amount of hydrochloric acid was added and then purged with nitrogen gas to remove sulfide. Gas compositions in the influent, inside of the column from the gas sampling port, and the off gas were determined by a gas chromatograph equipped with thermal conductivity detector (Shimadzu GC-14BPT). Acetate and propionate concentrations of influent and effluent were measured using a gas chromatograph equipped with flame ionization detector (Shimadzu GC-14BPF). At the end of each operational phase, sludge samples were collected from the upper, middle, and lower parts of the reactor sponge and used for further analysis. Dissolved CH_4 in the influent and effluent was measured by the headspace technique described previously (Hatamoto et al., 2010). Dissolved methane concentration was calculated based on Henry's Law using quantities of equilibrated headspace methane and Bunsen's coefficient. Concentrations of suspended solids and volatile suspended solids (VSS) in the retained sludge were determined according to the standard method (APHA-AWWA-WEF, 1995).

Elemental sulfur was extracted from sludges with acetone as the solvent in an ultrasonic water bath for 1 h. The concentration of elemental sulfur was determined using high performance liquid chromatography (HPLC LC-10A; Shimadzu, Kyoto, Japan) with a COSMOSIL type 5C₁₈-AR-II column (Nacalai Tesque, Kyoto, Japan) and UV detector (SPD-10AVvp; Shimadzu Co., Kyoto, Japan). The mobile phase was methanol at a flow rate of 1 ml·min⁻¹ and sulfur was detected at 230 nm.

The calculations for flow and removal rate were based on sponge volume. Oxygen consumption rates of CH₄, NH₄⁺, and sulfide oxidations were calculated based on the theoretical oxygen demands of 4 g-O₂·g-CH₄⁻¹, 4.57 g-O₂·g-N⁻¹, and 1.5 g-O₂·g-S⁻¹ from the CH₄ and NH₄⁺ removal rate and SO₄²⁻ production rate, respectively.

2.3 Cloning and sequencing of the 16S rRNA gene and phylogenetic analysis

Sludge samples were squeezed and collected from the upper, middle, and lower parts of the reactor sponge and washed with phosphate buffer. DNA was extracted from the washed sludges using the Fast DNA spin kit for soil (MP Biomedicals, Irvine, CA), as described in the manufacturer's instructions. Extracted DNA was used for amplification of bacterial 16S rRNA gene fragments with primer pairs of EUB338F/1492R (Hatamoto et al., 2007). Three clone libraries were constructed using previously described methods (Hatamoto et al., 2010). The cloned 16S rRNA gene fragments were sequenced at the Dragon Genomics Center (TAKARA BIO, Yokkaichi, Japan). Chimeric sequences were identified and removed using the Bellerophon program (Huber et al., 2004). 16S rRNA gene sequences with ≥97% identity were grouped into the same phylogenetic clone type by using the FastGroupII program (Yu

et al., 2006). The ribosomal database project classifier tool was employed to assign the 16S rRNA genes to appropriate taxonomic groups (Wang et al., 2007). Phylogenetic analysis using the ARB program was also performed for poorly classified sequences.

2.4 T-RFLP analysis of *pmoA* genes

Sludge collection and DNA extraction was performed as described above. PCR amplification of the *pmoA* gene was done with primer pairs of A189f labeled with Beckman-dye D4 and mb661 (Costello and Lidstrom, 1999). PCR reaction was initiated with 5 min of initial denaturation at 94 °C and 25 cycles of 30 s at 94 °C, 30 s at 56 °C, and 1 min at 72 °C. The final extension step was at 72 °C for 4 min. The PCR products were digested by MspI restriction endonuclease. Digested samples were analyzed on the CEG-2000XL (Beckman Coulter, Fullerton, CA) as described previously (Hatamoto et al., 2008).

2.5 Statistical analysis of the T-RFLP patterns

The terminal restriction fragment (T-RF) data of the *pmoA* gene was used for multidimensional scaling (MDS) statistical analyses according to a previous report (Yamada et al., 2008). Briefly, the relative abundances of each T-RF fragment were normalized by calculating the proportion of a given peak height to the total peak height. The small T-RF peaks, e.g. peak height below 100 relative fluorescence units or peak area below 1% of the total area, were removed as background noise. The bp numbers of T-RFs having the decimal numbers rounded to whole numbers. MDS analyses were performed using the Bray–Curtis coefficient based on the relative abundance of the peak height of the T-RFs with PASW

statistics 18 software (IBM, Somers, NY, USA).

3. Results and Discussion

3.1 Reactor performance

In this study, to investigate the influence of airflow rate and HRT on the reactor performance, the closed DHS reactor was operated under five different conditions (two HRT conditions and four airflow rate conditions). The operational parameters and average performance of the reactor are summarized in Table 1, and the results of the continuous experiment are shown in Fig. 2. In phase 1, methane removal efficiency decreased sharply to below 10% within 3 weeks of reactor start up. As with methane removal, ammonium removal also decreased and ceased in phase 1. Meanwhile, nearly the entire amount of influent sulfide was oxidized to sulfate, and steady sulfide oxidation was continued to phase 4 even though operational conditions were changed. More than 90% of influent organic substrates of acetate and propionate were also removed (effluent concentrations of acetate and propionate below 1.6 and 0.5 mg·L⁻¹, respectively), and total COD removal was maintained around 80% up to phase 4 (Table 1). In phase 2, the air supply rate was increased, and then, methane removal was drastically increased to 80%. However, the ammonium concentration in the effluent remained unchanged; thus, apparent ammonia oxidation did not occur at the increased air supply rate (Fig. 2). The air supply rate was further increased in phase 3, while the methane removal ratio was temporarily dropped but recovered to values greater than 90%. The ammonium removal rate also increased, and a corresponding increase in nitrate concentration in the effluent was observed. In addition, nitrite was not detected in the effluent

throughout the experiment. At the end of phase 3, the nitrate production rate was lower than the ammonium removal rate of about $0.5\text{--}0.9\text{ kg-N}\cdot\text{m}^{-3}\cdot\text{day}^{-1}$, indicating denitrification. The average methane and ammonium removal rates in phase 3 were $0.5\text{ kg-COD}\cdot\text{m}^{-3}\cdot\text{day}^{-1}$ and $0.31\text{ kg-N}\cdot\text{m}^{-3}\cdot\text{day}^{-1}$, respectively.

Although the HRT was decreased to 1 h in phase 4, it had little effect on sulfide oxidation and COD removal (Table 1, Fig. 2). However, the ammonium removal rate decreased sharply immediately following the reduction of the HRT, and the ammonium removal rate gradually decreased to below 10% thereafter. The methane removal ratio also decreased to below 50% in the start of phase 4; however, further decrease was not observed during that phase (Fig. 2). In phase 5, the HRT was the same as that in phase 4, but the air supply rate was decreased further; thus, methane and ammonium removal almost ceased; furthermore, sulfate production decreased and COD removal also deteriorated to approximately 50% (Fig. 2, Table 1). In this phase, oxygen concentration in the reactor off-gas decreased to 3% and elemental sulfur accumulated on the DHS sponge carriers. The average accumulated amounts of sulfur in the upper, middle, and lower parts of the reactor sponge carriers were 1950, 2460, and 180 $\text{mg-S}\cdot\text{L}^{-1}\cdot\text{sponge}$, respectively. The average sludge concentrations at the end of phase 4 were 13.3, 10.8, and 6.3 $\text{g-VS}\cdot\text{L}^{-1}\cdot\text{sponge}$, for the upper, middle, and lower parts of the sponge carriers, respectively.

3.2 Oxygen consumption of the reactor

The oxygen based air supply rate and average oxygen consumption rates in each operational phase calculated based on methane, ammonium, COD, and sulfide oxidation are shown in

Fig. 3. Under the same HRT condition of phases 1 to 3, the total oxygen consumption rate increased, corresponding to the increase in the air supply rate. Steady removal of COD and sulfide was observed and their oxygen consumption rates were almost stable in this phase. So, the increase in oxygen consumption resulted primarily from the increase in methane and ammonia oxidation in phases 2 and 3, respectively (Fig. 3). In the subsequent phase, the air supply rate was fixed and the influent flow rate of artificial wastewater was increased with an HRT of 1 h. The oxygen consumption rate of COD and sulfide oxidation correspondingly increased, and ammonia oxidation diminished. The total oxygen consumption rate was therefore almost the same in the phases 3 and 4 and the rate was around $2.5 \text{ kg-O}_2\cdot\text{m}^{-3}\cdot\text{day}^{-1}$. In phase 3, most of the supplied substrates were oxidized, but in phase 4, unoxidized methane and ammonium remained and the total oxygen consumption rate accounted for 64% of the supplied oxygen. Thus, the total oxygen consumption rate of about $2.5 \text{ kg-O}_2\cdot\text{m}^{-3}\cdot\text{day}^{-1}$ could be the limit of oxygen uptake of the DHS reactor.

The total oxygen consumption rate of the reactor was around $2.5 \text{ kg-O}_2\cdot\text{m}^{-3}\cdot\text{day}^{-1}$, a value in agreement with that in previous reports (Hatamoto et al., 2010; Machdar et al., 1997; Tandukar et al., 2007). The upper limit of the aerobic treatment system of the DHS reactor is therefore confirmed again as being approximately $2.5 \text{ kg-O}_2\cdot\text{m}^{-3}\cdot\text{day}^{-1}$, which includes the dissolved methane oxidation as well. Using this value as a benchmark, we may determine the appropriate DHS reactor volume according to the water quality of anaerobically treated effluent and could make a post-treatment system for preventing greenhouse gas emission.

From the oxygen consumption rate in the reactor (Fig. 3), ammonia oxidation showed the greatest variation, indicating that it was dependent on variations in operational condition.

The possible reasons for sensibility of ammonia oxidation are low oxygen affinity of ammonia-oxidizing bacteria (Bodelier and Laanbroek, 1997; Satoh et al., 2000) and lower free energy change of ammonia oxidation compared to acetate, propionate, methane, and sulfide oxidations (Rittmann & McCarty, 2001). Microbial growth yield is correlated to the catabolic free energy (Roden & Jin, 2011; VanBriesen, 2002), and the low growth yield of ammonia-oxidizing bacteria is well-known things (Rittmann & McCarty, 2001). Thus ammonia-oxidizing bacteria lose competition with other bacteria for oxygen under oxygen-limited condition. Therefore, ammonia-oxidizing bacteria could not maintain the appropriate population and the ammonium removal rate gradually decreased in phase 4 (Fig.2C).

Sulfur-oxidizing bacteria have been reported to show high affinity for oxygen (Overmann and Pfennig, 1992), and in a previous study, sulfide oxidation primarily occurred even under low oxygen conditions (Matsuura et al., 2010). Our results indicate that sulfide oxidation also occurred preferentially. Organic matter oxidation also occurred preferentially in our experiment. Heterotrophic bacteria have lower half-saturation constants for oxygen than ammonia-oxidizing bacteria, so heterotrophic bacteria outcompete ammonia oxidizers in oxygen-limited or organic carbon-rich conditions (Bodelier and Laanbroek, 1997; Satoh et al., 2000). For competition of oxygen between methane-oxidizing bacteria and heterotrophic bacteria, Shen et al. (1996) reported that methanotrophs of *Methylosinus sporium* might not have sufficient oxygen affinity to compete with heterotrophs under oxygen limited conditions. On the contrary, van Bodegom et al. (2001) reported that methane-oxidizing bacteria were able to outcompete heterotrophic bacteria only at low oxygen concentrations;

however, they also reported that high acetate concentration inhibited methane oxidation. In this study, organic matter decomposition occurred in preference to methane oxidation, which might be attributed to the fact that acetate and propionate were used as organic substrates.

3.3 Microbial community analysis

The microbial community structures of various wastewater treatment systems have been well studied using molecular techniques. However, little is known about the microbial community structure of dissolved methane oxidizing wastewater treatment process. In this study, therefore we conducted the 16S rRNA gene based microbial community analysis using DNA extracted from the sludges obtained on the day 120 (phase 3), which phase exhibited the best treatment performance during the entire reactor operation. The microorganisms belonging to *Betaproteobacteria*, *Gammaproteobacteria*, and *Bacteroidetes* dominated in the clone libraries (Table 2). These microorganisms were dominant in aerobic wastewater treatment system (Wagner & Loy, 2002), and also predominant in other DHS reactor (Kubota et al., 2010; Okawara et al., 2010). Methane-oxidizing bacterial species were detected only in upper and middle parts of the reactor and accounted for 6.4 and 2.2% of total clones, respectively (Table 2). These percentages were much lower than the percentages of 30–50% obtained in our previous study using methane and ammonium as substrates (Hatamoto et al., 2010). As for the sulfur-oxidizing bacteria, the *Thiobacillus* species (5 clones in the upper part) and *Sulfuricurvum* species (2 clones in the lower part) were detected. In addition, nitrifying bacteria of genera *Nitrosomonas*, *Nitrosospira*, and *Nitrospira* were detected in the upper and middle parts of the reactor.

To characterize the succession of methanotrophic communities, we first analyzed on the *pmoA* gene targeted T-RFLP analysis using sludge samples taken from the upper, middle, and lower parts of the reactor at the end of each phase (phase 1, day 30; phase 2, day 78; phase 3, day 120; phase 4, day 163; phase 5, day 197) (Supplementary Fig. S1). Then, MDS statistical analyses were performed by using data sets of the T-RFLP profile (Fig. 4). The result of the MDS analysis for the DHS reactor indicated that the methanotrophic community structures were divided roughly into three groups. The group consisting of phase 1, phase 2, and the upper part of phase 3 represented the early stages of the experiment. Other groups including the middle parts of phases 3, 4, and 5 and the lower parts of phases 4 and 5 consisted of samples from later stages of the experiment. The characteristic T-RF peak of the former group was 244 bp, which represented type II of methanotrophs. The latter group had a characteristic T-RF peak of 77 bp, which represented type I methanotrophs of the *Methylocaldum* species (Supplementary Fig. S1). The results showed that quite different methanotrophic communities were formed in the DHS reactor operation.

Methane-oxidizing bacterial communities gradually changed from the start up period to later operational phases, which were mostly composed of type I methanotrophs of the *Methylocaldum* species. The operational conditions of the later operational phases 4 and 5 are quite different, but their methanotrophic bacterial communities were not drastically altered (Fig. 4). *Methylocaldum* species were also dominant methanotrophs in our previous dissolved methane oxidizing DHS reactor study (Hatamoto et al, 2010), thus the methanotrophs could be an important species for dissolved methane oxidation. In addition, the process performance responded relatively quick to changes in operational conditions, but

successions of microbial communities took a longer time to respond, which might be attributed to the higher sludge retention time of a DHS reactor (Tandukar et al., 2007).

4. Conclusions

Experiments were conducted using a closed DHS reactor to treat an artificially prepared anaerobically treated wastewater effluent to gain basic understanding of a post-treatment system that prevents methane emission during anaerobic wastewater treatment. The results obtained confirmed that the limitation of the DHS reactor was approximately 2.5 $\text{kg-O}_2\cdot\text{m}^{-3}\cdot\text{day}^{-1}$. Under that condition, oxidation of sulfides and organic matter primarily occurred; then, methane was oxidized, and finally, ammonia oxidation occurred if residual oxygen was present.

Acknowledgments

This research was supported by a Grant-in-Aid for the “Development of High-efficiency Environmental Biotreatment Technology using Artificially Designed Microbial Communities” project from the New Energy and Industrial Technology Development Organization (NEDO).

References

APHA-AWWA-WEF, 1995. Standard Methods for the Examination of Water and Wastewater. 19th ed., American Public Health Association, Washington, DC, USA

- Bodelier, P.L.E., Laanbroek, H.J., 1997. Oxygen uptake kinetics of *Pseudomonas chlororaphis* grown in glucose- or glutamate-limited continuous cultures. *Arch. Microbiol.*, 167, 392-395.
- Costello, A.M., Lidstrom, M.E. 1999. Molecular characterization of functional and phylogenetic genes from natural populations of methanotrophs in lake sediments. *Appl. Environ. Microbiol.*, **65**, 5066-5074.
- Forster, P., Ramaswamy, V., Artaxo, P., Berntsen, T., Betts, R., Fahey, D.W., Haywood, J., Lean, J., Lowe, D.C., Myhre, G., Nganga, J., Prinn, R., Raga, G., Schulz, M., van Dorland, R., 2007. Changes in Atmospheric Constituents and in Radiative Forcing. in: S. Solomon, D. Qin, M. Manning, Z. Chen, M. Marquis, K.B. Averyt, M. Tignor, H.L. Miller (Eds.), *Climate change 2007: The physical science basis. Contribution of working group I to the fourth assessment report of the intergovernmental panel on climate change*. Cambridge University Press, Cambridge, United Kingdom and New York, NY, USA.
- Hartley, K., Lant, P., 2006. Eliminating non-renewable CO₂ emissions from sewage treatment: An anaerobic migrating bed reactor pilot plant study. *Biotechnol. Bioeng.*, 95, 384-398.
- Hatamoto, M., Imachi, H., Ohashi, A., Harada, H., 2007. Identification and cultivation of anaerobic, syntrophic long-chain fatty acid-degrading microbes from mesophilic and thermophilic methanogenic sludges. *Appl. Environ. Microbiol.*, 73, 1332-1340.

- Hatamoto, M., Imachi, H., Yashiro, Y., Ohashi, A., Harada, H., 2008. Detection of active butyrate-degrading microorganisms in methanogenic sludges by RNA-based stable isotope probing. *Appl. Environ. Microbiol.*, 74, 3610-3614.
- Hatamoto, M., Yamamoto, H., Kindaichi, T., Ozaki, N., Ohashi, A., 2010. Biological oxidation of dissolved methane in effluents from anaerobic reactors using a down-flow hanging sponge reactor. *Water Res.*, 44, 1409-1418.
- Huber, T., Faulkner, G., Hugenholtz, P., 2004. Bellerophon: a program to detect chimeric sequences in multiple sequence alignments. *Bioinformatics*, 20, 2317-2319.
- Kassab, G., Halalsheh, M., Klapwijk, A., Fayyad, M., van Lier, J.B., 2010. Sequential anaerobic-aerobic treatment for domestic wastewater - A review. *Bioresour. Technol.*, 101, 3299-3310.
- Kubota, K., Hayashi, M., Matsunaga, K., Ohashi, A., Li, Y.-Y., Yamaguchi, T., Harada, H., 2010. Microbial community structure of G3-DHS reactor in UASB-DHS system treating domestic sewage. *Doboku Gakkai Ronbunshuu G*, 66, 56-64 (in Japanese with English abstract).
- Machdar, I., Faisal, M., 2011. Modification of DHS bioreactor module with oil palm fiber material for treating domestic wastewater. *J. Water Environ. Technol.*, 9, 47-52.
- Machdar, I., Harada, H., Ohashi, A., Sekiguchi, Y., Okui, H., Ueki, K., 1997. A novel and cost-effective sewage treatment system consisting of UASB pre-treatment and aerobic post-treatment units for developing countries. *Wat. Sci. Technol.*, 36, 189-197.

- Matsuura, N., Hatamoto, M., Sumino, H., Syutsubo, K., Yamaguchi, T., Ohashi, A., 2010. Closed DHS system to prevent dissolved methane emissions as greenhouse gas in anaerobic wastewater treatment by its recovery and biological oxidation. *Water Sci Technol.*, 61, 2407-15.
- Okawara, M., Hatamoto, M., Nishiyama, K., Matsuura, N., Abe, H., Syutsubo, K., Imachi, H., Harada, H., Yamaguchi, T., Ohashi, A., 2010 Recovery of dissolved methane in effluent of anaerobic wastewater treatment by closed DHS unit. *J. Japan Society on Water Environ.*, 33, 25-31 (in Japanese with English abstract).
- Overmann, J., Pfennig, N., 1992. Continuous chemotrophic growth and respiration of Chromatiaceae species at low oxygen concentrations. *Arch. Microbiol.*, 158, 59-67.
- Rittmann, B.E., McCarty, P.L. 2001. Environmental biotechnology: Principles and applications. McGraw-Hill, New York, NY.
- Roden, E.E., Jin, Q. 2011. Thermodynamics of microbial growth coupled to metabolism of glucose, ethanol, short-chain organic acids, and hydrogen. *Appl. Environ. Microbiol.*, 77, 1907-1909.
- Satoh, H., Okabe, S., Norimatsu, N., Watanabe, Y., 2000. Significance of substrate C/N ratio on structure and activity of nitrifying biofilms determined by in situ hybridization and the use of microelectrodes. *Wat. Sci. Technol.*, 41, 317-321.
- Shen, C., Miguez, C., Bourque, D., Groleau, D., Guiot, S., 1996. Methanotroph and methanogen coupling in granular biofilm under O₂-limited conditions. *Biotechnol. Lett.*, 18, 495-500.

- Takahashi, M., Yamaguchi, T., Kuramoto, Y., Nagano, A., Shimozaki, S., Sumino, H., Araki, N., Yamazaki, S., Kawakami, S., Harada, H., 2011. Performance of a pilot-scale sewage treatment: An up-flow anaerobic sludge blanket (UASB) and a down-flow hanging sponge (DHS) reactors combined system by sulfur-redox reaction process under low-temperature conditions. *Bioresource. Technol.*, 102, 753-757.
- Tandukar, M., Ohashi, A., Harada, H., 2007. Performance comparison of a pilot-scale UASB and DHS system and activated sludge process for the treatment of municipal wastewater. *Water Res.*, 41, 2697-2705.
- van Bodegom, P., Stams, F., Mollema, L., Boeke, S., Leffelaar, P., 2001. Methane oxidation and the competition for oxygen in the rice rhizosphere. *Appl. Environ. Microbiol.*, 67, 3586-3597.
- VanBriesen, J.M. 2002. Evaluation of methods to predict bacterial yield using thermodynamics. *Biodegradation*, 13, 171-190.
- Wagner, M., Loy, A. 2002. Bacterial community composition and function in sewage treatment systems. *Curr. Opin. Biotechnol.*, 13, 218-227.
- Wang, Q., Garrity, G.M., Tiedje, J.M., Cole, J.R., 2007. Naive bayesian classifier for rapid assignment of rRNA sequences into the new bacterial taxonomy. *Appl. Environ. Microbiol.*, 73, 5261-5267.
- Yamada, T., Suzuki, A., Ueda, H., Ueda, Y., Miyauchi, K., Endo, G., 2008. Successions of bacterial community in composting cow dung wastes with or without hyperthermophilic pre-treatment. *Appl. Microbiol. Biotechnol.*, 81, 771-781.

Yu, Y., Breitbart, M., McNairnie, P., Rohwer, F., 2006. FastGroupII: A web-based bioinformatics platform for analyses of large 16S rDNA libraries. *BMC Bioinformatics*, 7, 57.

Figure legends

Fig. 1 Schematic diagram of the closed DHS reactor. The artificial wastewater is purged with pure methane gas to ensure a 100% methane atmosphere.

Fig. 2 Operational conditions and process performance of the closed DHS reactor. (a) Influent dissolved methane loading rate, methane removal rate, and methane removal ratio. (b) Methane and oxygen concentrations of exhaust gas. (c) Ammonium loading and removal rates and nitrate production rate. (c) Sulfide loading and sulfate production rates. Methane removal is calculated based on quantities of influent dissolved methane and total effluent methane (dissolved methane in exhaust off-gas plus dissolved methane in effluent).

Fig. 3 Oxygen consumption and supply rate in each operational phase. The oxygen consumption rate is calculated from average methane, ammonia, COD removal, and sulfate production rates. The error bars indicate the standard deviations.

Fig. 4 Succession in the methanotrophic bacterial community structure of closed DHS retained sludge evaluated by multidimensional scaling analysis. The sludge samples were taken from upper, middle, and lower parts of the reactor at each end of the operational phase.

Table 1 Operational parameters and summary of the process performance

Parameter	Unit	Phase				
		1	2	3	4	5
Operational period	day	1–29	30–78	79–119	120–162	163–197
HRT	hour	2	2	2	1	1
Air flow rate	L day ⁻¹	0.88	1.43	3.21	3.21	0.79
Inf. dissolved CH ₄ conc.	mg-COD · L ⁻¹	58.4 (4.2)	56.0 (6.2)	60.8 (5.3)	59.8 (4.4)	66.5 (4.5)
Eff. total CH ₄ conc. ^a	mg-COD · L ⁻¹	38.9 (17.6)	14.7 (6.7)	12.8 (10.8)	34.8 (5.5)	57.5 (10.3)
Inf. total COD conc.	mg-COD · L ⁻¹	52.6 (7.5)	58.7 (7.1)	56.2 (8.9)	59.1 (4.7)	61.3 (2.6)
Eff. COD conc.	mg-COD · L ⁻¹	3.4 (2.7)	13.4 (5.4)	13.8 (8.5)	12.0 (3.3)	34.5 (5.2)
Inf. NH ₄ ⁺ conc.	mg-N · L ⁻¹	36.2 (3.4)	34.0 (2.9)	37.6 (4.0)	40.1 (2.7)	39.3 (2.4)
Eff. NH ₄ ⁺ conc.	mg-N · L ⁻¹	31.5 (5.4)	30.0 (3.6)	7.7 (6.2)	31.6 (4.8)	38.8 (2.4)
Eff. NO ₃ ⁻ conc.	mg-N · L ⁻¹	2.2 (4.8)	2.7 (1.7)	26.2 (6.2)	4.7 (3.9)	0.1 (0.5)
Eff. SO ₄ ²⁻ conc.	mg-S · L ⁻¹	22.0 (6.0)	20.4 (5.6)	18.4 (2.7)	17.2 (1.8)	9.3 (3.2)

The numbers in parentheses are standard deviations.

^a Effluent methane concentration is calculated from the influent flow rate and total quantities of methane in exhaust off-gas plus dissolved methane in effluent.

Table 2 Bacterial 16S rRNA gene clones retrieved from the closed DHS retained sludges.

Phylogenetic affiliation	No. of clones (% of total clones)		
	Upper	Middle	Lower
<i>Alphaproteobacteria</i>			
<i>Methylocystis</i>	3 (3.2)	1 (1.1)	
other			
<i>Alphaproteobacteria</i>	5 (5.3)	22 (23.7)	3 (4.3)
<i>Betaproteobacteria</i>			
<i>Thiobacillus</i>	5 (5.3)		
<i>Nitrospira</i>	3 (3.2)	2 (2.2)	
<i>Nitrosomonas</i>	1 (1.1)	2 (2.2)	
other <i>Betaproteobacteria</i>	15 (16.0)	8 (8.6)	26 (37.1)
<i>Gammaproteobacteria</i>			
<i>Methylobacter</i>	2 (2.1)		
<i>Methylosarcina</i>	1 (1.1)		
<i>Methylocaldum</i>		1 (1.1)	
other			
<i>Gammaproteobacteria</i>	10 (10.6)	6 (6.5)	3 (4.3)
<i>Deltaproteobacteria</i>	1 (1.1)	3 (3.2)	6 (8.6)
<i>Epsilonproteobacteria</i>			
<i>Sulfuricurvum</i>			2 (2.9)
other			
<i>Epsilonproteobacteria</i>			3 (4.3)
<i>Acidobacteria</i>	11 (11.7)	3 (3.2)	5 (7.1)
<i>Bacteroidetes</i>	18 (19.1)	25 (26.9)	17 (24.3)
<i>Chloroflexi</i>	12 (12.8)	4 (4.3)	1 (1.4)
<i>Nitrospira</i>	5 (5.3)	5 (5.4)	
<i>Verrucomicrobia</i>		5 (5.4)	
Other	2 (2.1)	6 (6.5)	4 (5.7)
Total	94 (100)	93 (100)	70 (100)

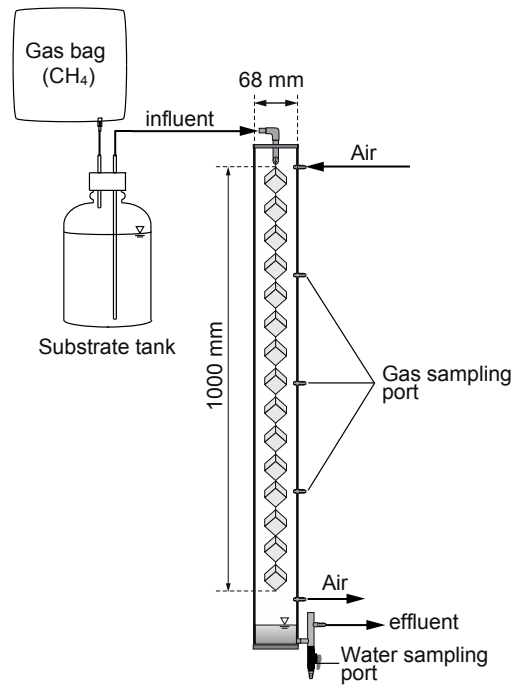


Fig. 1 Schematic diagram of the closed DHS reactor. The artificial wastewater is purged with pure methane gas to ensure a 100% methane atmosphere.

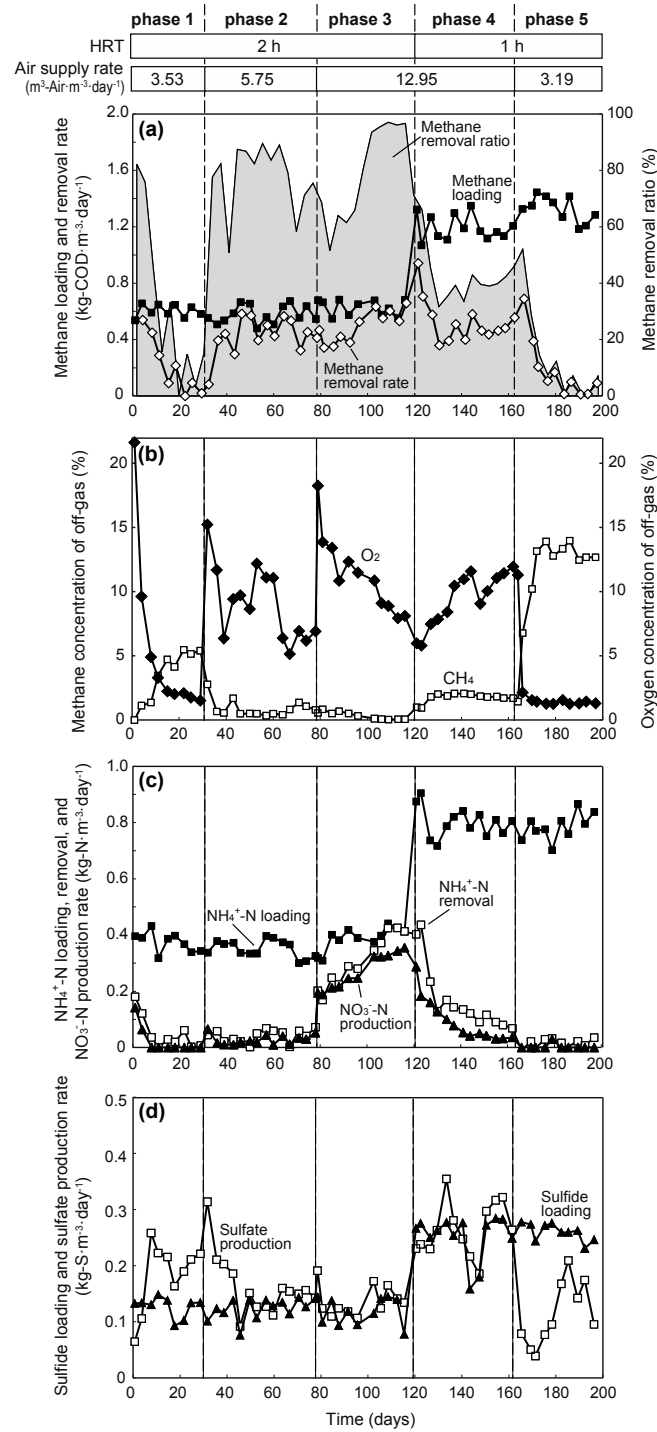


Fig. 2 Operational conditions and process performance of the closed DHS reactor. (a) Influent dissolved methane loading rate, methane removal rate, and methane removal ratio. (b) Methane and oxygen concentrations of exhaust gas. (c) Ammonium loading, removal and nitrate production rates. (c) Sulfide loading and sulfate production rates. Methane removal is calculated based on quantities of influent dissolved methane and total effluent methane (dissolved methane in exhaust off-gas plus dissolved methane in effluent).



Fig. 3 Oxygen consumption and supply rate at each operational phase. Oxygen consumption rate is calculated from average methane, ammonia, and COD removal and sulfate production rates. Error bars indicate the standard deviations.

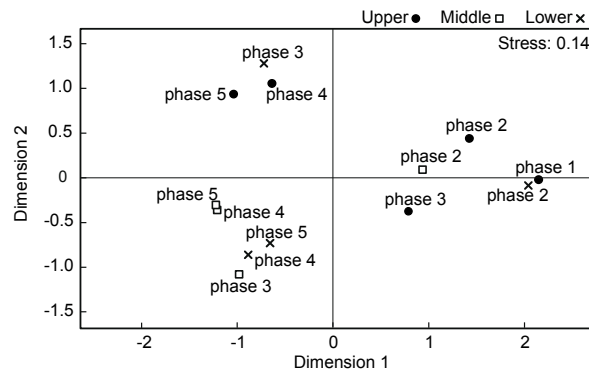


Fig. 4 Succession in the methanotrophic bacterial community structure of closed DHS retained sludge evaluated by multidimensional scaling analysis. The sludge samples were taken from upper, middle, and lower parts of the reactor at each end of operational phase.